

Charged-particle multiplicity distribution in limited rapidity windows in hadron-nucleus scattering

Y. P. Chan and K. Young

Department of Physics, The Chinese University of Hong Kong, Hong Kong

D. Kiang and T. Ochiai

Department of Physics, Dalhousie University, Halifax, Nova Scotia, Canada B3H 3J5

(Received 2 April 1990)

The charged-particle multiplicity distributions in different limited rapidity windows obtained in hadron-nucleus scattering at 200–360 GeV are examined using a model built from three general ideas: the geometric model, thermodynamic concepts, and independent emission of charged pairs. The model fits the data very well, especially for the distribution of negative charges, which does not suffer from contamination by protons “evaporated” from the nucleus. A central ingredient in the thermodynamic concept is the conservation of momentum in the collision of the beam hadron with an effective target, the latter being a tube of $\sim \nu$ particles. It is suggested that all dynamical models with $\sim \nu$ collisions and conservation of momentum would give similar results, and that this is the reason for the success of different dynamical models applied to this problem.

I. INTRODUCTION

High-energy hadron-nucleus (hA) scattering has been studied for some two decades because it yields information on the space-time development of hadronic interactions,¹ and on reaction channels which are not directly accessible, e.g., elastic scattering of resonances,² or the absorption of particular components of the hadronic wave function in nuclear matter.³ The possibility of a phase transition in hadronic matter is particularly intriguing,⁴ and provides the impetus for recent interest in heavy-ion collisions.⁵ Because the dynamics of hA scattering is complex and large numbers of particles are produced, much of the experimental data refer to integrated quantities such as the multiplicity or the one-particle distribution. The initial interest concentrated on (a) the total number of charged particles n , with mean \bar{n} and distribution $P(n)$,^{6–9} and also on (b) the total number of negative charges n_- , with mean \bar{n}_- and distribution $P_-(n_-)$.⁸ The latter does not suffer from contamination by protons knocked out from the nucleus. More detailed information has recently been obtained by restricting attention to certain rapidity windows Δy , and considering (c) the number of charged particles m , with mean $\bar{m}(\Delta y)$ and distribution $P(m, \Delta y)$,^{10,11} and (d) the analogous distribution $P_-(m_-, \Delta y)$ for the negative charges only.¹⁰ The information on $\bar{m}(\Delta y)$ is in principle identical to the one-particle distribution.

The experiments which will be referred to in this paper are summarized in Table I. Of the many experimental results for the full rapidity window,^{6–9} we select only Ref. 8 which used the same experimental setup as in the recent experiment¹⁰ on limited rapidity windows.

Integrated quantities such as the multiplicity, though in a sense mundane, nevertheless require theoretical understanding, if only to provide benchmark expectations,

departures from which might signify more exotic phenomena such as a quark-gluon-plasma phase.⁴ The charged multiplicity and the negative multiplicity, both in the full and in restricted rapidity windows, have been described by a multisource statistical model.¹² The VENUS model¹³ based on color exchange and string formation and fragmentation accounts reasonably well for all features (a)–(d) of the data. Geometric ideas combined with the wounded-nucleon model also agree quite well with the data, except for large rapidity windows in the backward hemisphere.¹⁴ The geometric branching model¹⁵ and the Lund FRITIOF model¹¹ have also been used to describe hA multiplicities. The fact that these models, with different dynamical assumptions, have all been successful to some degree would argue that the experimental data are only sensitive to and serve only to confirm certain common ingredients, which do not involve dynamical details.

In this paper, we attempt to identify three main ideas which are broadly accepted and implicit in virtually all models considered, and to show that the synthesis of these ideas, without further dynamical assumptions, leads naturally to a satisfactory description of all aspects of the data (a)–(d). It must be stressed that in doing so we do not in any way challenge the various models hitherto advanced, but rather complement them by highlighting the ingredients that are, in our view, most stringently tested by the data.

TABLE I. Summary of experimental measurements.

Reaction	Energy/ A (GeV)	Measurements	Ref.
$p + \text{Xe}, \text{Ar}$	200	a, b	8
$p + \text{Xe}, \text{Ar}$	200	c, d	10
$p + \text{Au}, \text{Al}$	360	c	11

These three ideas are the geometric model which describes each collision as occurring at a specific value of the impact parameter b , the partition-temperature model which provides a thermodynamic description of the one-particle distribution, subject to certain conservation laws, and the idea of independent emission of final-state particles. Section II presents the formalism incorporating these ideas, and Sec. III discusses the comparison with the data. The concluding remarks are in Sec. IV.

II. FORMALISM

A. Geometric model

Chiefly for the purpose of establishing notation, we first record the accepted ideas of the geometric model, essentially in the form used by us in the application to hA scattering.¹⁶ The geometric model is rooted in the eikonal approximation and the Glauber formalism,¹⁷ and relies on the small de Broglie wavelength of the projectile and the limited transverse momenta to associate a unique impact parameter b with each event, with observed quantities being an incoherent average over b , weighted by the inelastic cross section

$$d\sigma_i = d^2b(1 - e^{-\sigma t(b)}), \quad (1)$$

where σ is the inelastic p - p cross section, which in the range $5 \text{ GeV} < E < 1500 \text{ GeV}$ is conveniently described by¹⁸ $\sigma = \sigma_0(E/E_0)^\alpha$, where E is the energy in the laboratory frame, $\sigma_0 = 26.8 \text{ mb}$, $E_0 = 1 \text{ GeV}$, and $\alpha = 0.037$. In Eq. (1), $t(b)$ is the thickness of the tube of nuclear matter which acts as the effective target: $t(b) = \int dz \rho(r)$, $r = (z^2 + b^2)^{1/2}$. For medium and large nuclei ($A > 30$), the density ρ is given by the Woods-Saxon form, with standard values of the parameters as in Ref. 16, and normalized to the mass number A .

In traversing a tube of length $t(b)$, there will be, on the average, $\nu(b) = \sigma t(b)(1 - e^{-\sigma t(b)})^{-1}$ interactions, and the average of $\nu(b)$ over the whole nucleus is

$$\bar{\nu} = \int d\sigma_i \nu(b) / \int d\sigma_i = A\sigma / \sigma_i^{hA}. \quad (2)$$

The average multiplicity \bar{n} increases with the number of collisions, phenomenologically as¹⁹

$$\bar{n}(\bar{\nu}) = \bar{n}^{hN} [1 + k(\bar{\nu} - 1)], \quad (3)$$

where \bar{n}^{hN} is the charged multiplicity in p - p collisions, parametrized as²⁰

$$\bar{n}^{hN} = 1.2 + 0.59 \ln(E/E_0) + 0.12 [\ln(E/E_0)]^2 \quad (4)$$

and $k \sim 0.5$, with the precise value left open as a free parameter. A popular interpretation of (3) is that the first collision "wounds" the projectile,²¹ which is therefore less effective, by a factor k , in producing particles in the $\nu - 1$ subsequent collisions. Other interpretations are possible, especially if $k = \frac{1}{2}$, so that (3) is proportional to $1 + \nu$, with the first term representing the beam particle and the second term the ν particles in the target which interacted.^{14,21} It is natural to generalize (3) to each impact parameter

$$\bar{n}(b) = \bar{n}^{hN} \{1 + k[\nu(b) - 1]\} \quad (5)$$

whose average, weighted by $d\sigma_i$, would recover (3).

The observed fluctuation in the multiplicity n is largely due to the dispersion in $\bar{n}(b)$, and explains the Koba-Nielsen-Olesen- (KNO-) type behavior with $\Delta n \sim n$,²² as emphasized by many authors in the context of hh scattering.²³ Moreover, the fact that $\bar{n}(b)$ has a maximum at $b = 0$ accounts for a mild break observed in the multiplicity distribution in hh scattering at collider energies,²⁴ and a much more prominent one in heavy-ion collisions.^{5,25} All these considerations stress that, for a given b , the fluctuation of n around $\bar{n}(b)$ is of secondary importance, so that a relatively simple parametrization should suffice. Previously, we had assumed universal KNO scaling at each b ,¹⁶ namely, that the distribution at each b is described by

$$p(n, b) dn = \psi_0(\xi) d\xi, \quad (6)$$

where $\xi = n / \bar{n}(b)$ and $\psi_0(\xi)$ is a universal function, say, the Slattery form.²⁶ This assumption suffers from two drawbacks. First of all, there is evidence that the fluctuation of n around $\bar{n}(b)$ goes as $\Delta n / \bar{n} \propto \nu(b)^{-1/2}$,⁸ rendering a universal form such as (6) invalid. While this feature would be visible when events are segregated according to ν (as estimated from grey tracks, for example), it will be largely smeared out when averaged over the whole nucleus, as evidenced by the success of the approximation of universal KNO scaling at each impact parameter in comparison with data,^{7,9,16} and in the interest of simplicity we retain the universality approximation in this paper.

The second problem is more serious, especially for the distribution of n_- . For a given b , the effective colliding system consists of the incident hadron together with a tube of nuclear matter, with a total net charge $q(b)$, which is conserved and does not fluctuate. The distribution (6) would give events with n going down to zero, in particular, with $n < q(b)$, and thus $n_- = [n - q(b)]/2 < 0$, which would be nonsensical and in particular would not be "lost" in averaging over b . A natural resolution is to assume instead that the colliding system produces $q(b)$ positive charges together with τ neutral pairs, so that $n_+ = q(b) + \tau$, $n_- = \tau$, with τ distributed according to (6), where now $\xi = \tau / \bar{\tau}(b)$, and $\bar{\tau}(b) = [n(b) - q(b)]/2$. It remains to specify $q(b)$. The relevant tube of nuclear matter has a length $t(b)$ and an area $f\sigma$, where σ is the inelastic p - p cross section and $f \sim 1$ is a parameter to be specified. Thus

$$q(b) = 1 + (Z/A)f\sigma t(b) \quad (7)$$

in which the first term represents the charge of the beam hadron. This modification has no effect when applied to $\bar{p}p$ collisions, and only a very minor effect for the distribution of n in hA collisions.

These inputs define the geometric aspects of the model, and suffice to determine the distribution of n and n_- for the full rapidity interval. In particular the observed probability is obtained by averaging (6) over impact parameters

$$P(n) = \int d\sigma_i p(n, b) / \int d\sigma_i, \quad (8)$$

where the explicit form of $p(n, b)$ after the above modification to take account of charge conservation will not be explicitly displayed.

B. Thermodynamic description

To go from the total number of charged particles n to the number m in a rapidity window Δy requires knowledge of the particle distribution in n -particle phase space. Since there is little correlation, except at very small rapidity separations,²⁷ this information is to a large extent captured by the one-particle distribution,²⁸ for which we now provide a thermodynamic description. Thermodynamic ideas for dealing with high-energy collisions have a long history,²⁹ and is motivated by the consideration that, with a large number of particles, all states in phase space are "equally" probable, subject to energy constraints, the Lagrange multiplier enforcing which becomes the inverse temperature in a canonical ensemble. The successful application of this idea to hh scattering in the center-of-mass frame³⁰ requires several modifications: relativistic phase space d^3p/E ; a factor $\exp(-\alpha p_\perp)$, with $\alpha = 4.2 \text{ GeV}^{-1}$ (Ref. 31) in order to take account of the fact that the transverse momentum is limited; allowing a fraction $1-h$ of the total energy to be carried away by leading particles without thermalizing; and applying these prescriptions at each impact parameter. While in principle h should decrease with b ,³⁰ we shall, again for simplicity, take it as a constant for a given process. For the cases under consideration $h \sim 0.6-0.7$, the precise value being left open as the third fitting parameter.

However, one further ingredient is needed for hA scattering,³¹ namely, the conservation of the longitudinal momentum of the colliding system, enforced by a second Lagrange multiplier and resulting in an extra factor $\exp(\lambda p_z)$, so that the one-particle distribution is, for a given impact parameter,

$$dn = B e^{-\alpha p_\perp} e^{\lambda p_z - E/T} d^3p/E \quad (9)$$

in which B is fixed by normalization to $\bar{n}(b)$, and T by the requirement that the total energy in produced particles comes to hE_t , where $E_t = M + E_0$ is the total energy of the colliding system, consisting of a beam hadron of energy E_0 and an effective target of mass M . It remains to determine λ , for which it is most convenient to regard the expression $\lambda p_z - E/T$ in the exponential as the Lorentz transform of $-E^*/T^*$ in the center-of-mass frame, in which p_z should be symmetrically distributed, so that $1/T = \gamma/T^*$, $\lambda = \gamma\beta/T^*$, where β and γ are the usual parameters of the Lorentz transformation. It is easy to show that $M \approx (h/2\gamma^2)E_0$, where M is the mass of the effective target, here a tube: $M = f\sigma t(b)m_p$, with $f \sim 1$ being the same as in (7). This prescription then determines γ and β , and in turn λ , without further adjustable parameters. The details are given in Ref. 31 and need not be repeated here.

For central collisions or collisions with larger nuclei ($\sigma t \sim \nu$ relatively large), the large target mass M means

that the center-of-mass velocity is relatively small and the distribution of produced particles is shifted to smaller rapidities; in contrast, for more peripheral collisions or collisions with smaller nuclei ($\sigma t \sim \nu$ relatively small), the distribution would be centered around larger rapidities. This feature is seen explicitly by comparing the $p\text{Ar}$ and $p\text{Xe}$ data in Ref. 8. Thus the imposition of momentum conservation and the correct identification of the effective target mass are crucial in obtaining the main features of the one-particle rapidity distribution. It is important to note that the target must be regarded as a tube ($M \sim \sigma t m_p \sim A^{1/3} m_p$ in an average sense) and not a single nucleon ($M = m_p$) or the whole nucleus ($M = Am_p$).

Since the spirit of this paper is to abstract the features common to various dynamical models, it is appropriate to stress that the *kinematic* constraint due to the conservation of momentum is implicit in all dynamical models, and responsible for their success. For example, in the multiple-scattering model,³² the incoming hadron with energy E_0 is assumed to divide into ν subcollisions, each with typical energy E_0/ν hitting one nucleon. The distribution of produced particles is centered about the center-of-mass rapidity defined by E_0/ν hitting a target of mass m_p , which is identical with that defined by the total energy E_0 hitting a target of mass $\nu m_p \sim M$. The additive quark model³³ has a similar feature, provided one identifies the number of wounded quarks with ν . Indeed any model which contains ν collisions and conserves momentum in each will define the same center-of-mass frame and hence the same mean rapidity for the distribution of produced particles.

With the thermodynamic description in hand, it is now possible to calculate the mean number of charged particles in a given rapidity window Δy , for events at a given b :

$$\bar{m}(\Delta y, b) = \int_{\Delta y} dn, \quad (10)$$

where dn is the expression in (9), with parameters defined for each b as described above. The observed mean number is obtained by averaging over impact parameters, weighted by the interaction probability:

$$\bar{m}(\Delta y) = \int d\sigma_i \bar{m}(\Delta y, b) / \int d\sigma_i. \quad (11)$$

C. Independent emission

For events at a given b , the probability of any charged particle falling into the rapidity window Δy is

$$r(\Delta y, b) = \bar{m}(\Delta y, b) / \bar{n}(b). \quad (12)$$

If we assume that particles are emitted *independently* in clusters of s particles, then the probability of observing m particles when a total of n is emitted would be given by the binomial distribution

$$Q(m, n, \Delta y, b) = \frac{1}{s} \binom{n/s}{m/s} r^{m/s} (1-r)^{(n-m)/s}. \quad (13)$$

This idea is used by many authors,^{12,34} and the evidence is that $s=2$,³⁴ in accord with theoretical expectations.

Thus the observed probability for m particles is

$$P(m, \Delta y) = \int d\sigma_i \sum_n Q(m, n, \Delta y, b) p(n, b) / \sigma_i^{hA}. \quad (14)$$

The discussion for negative charges is similar, except that $s=1$, since each cluster contains two charged particles but only one negative charge. With these formulas, all the quantities (a)–(d) discussed in the Introduction can be calculated.

This last part of the formalism can stand alone from the previous sections, if we make the approximation that r is independent of b , and replace (12) by

$$r(\Delta y) = \bar{m}(\Delta y) / \bar{n} \quad (15)$$

in which $\bar{m}(\Delta y)$ is given by (11) and similarly $\bar{n} = \int d\sigma_i \bar{n}(b) / d\sigma_i$, or, more directly, with $\bar{m}(\Delta y)$ and \bar{n} simply taken from the data. Then in (14) the factor Q can be taken out of the integral, and using (8), we obtain

$$P(m, \Delta y) = \frac{1}{s} \sum_n \binom{n/s}{m/s} r^{m/s} (1-r)^{(n-m)/s} P(n). \quad (16)$$

This approximate formalism was used in Refs. 12 and 34, but since we have to segregate different impact parameters anyway, we shall use (14), which is more appropriate.

III. COMPARISON WITH DATA

To summarize, three parameters need to be specified: $f \sim 1$ expressing the area of the effective target, the fraction $h \sim 0.6-0.7$ of the energy which thermalizes, and $k \sim 0.5$ expressing the reduced production of particles for

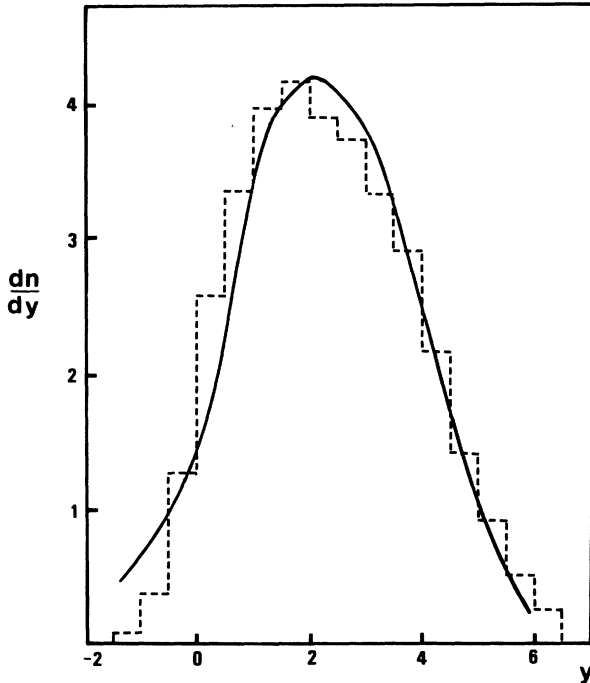


FIG. 1. Rapidity distribution dn/dy for $p + \text{Xe}$ scattering at 200 GeV. The histogram is the experimental data of Ref. 8, and the solid line is the fitted result of the present model with $f=1.3$, $h=0.7$, and $k=0.544$.

collisions other than the first. However, only minor adjustments are permitted, within the range indicated, and our results are largely independent of such adjustments. The parameter k is used in all theoretical models.

Consider the reaction $p + \text{Xe}$ at 200 GeV (Refs. 8 and 10) as an example; the case of $p + \text{Ar}$ is similar and will not be presented. The parameters chosen are $f=1.3$, $h=0.7$, $k=0.544$. Figure 1 shows the calculated one-particle rapidity distribution compared with the data;⁸ the fit is very good.

Figure 2 shows the mean multiplicity $\bar{m}(\Delta y)$ for various windows Δy , compared with the data.¹⁰ These windows are defined with respect to y_c , the “center-of-mass” rapidity calculated kinematically by assuming the target to be a single nucleon: $y_c=3.0$ in this case, so that an interval Δy in the forward/backward hemisphere means

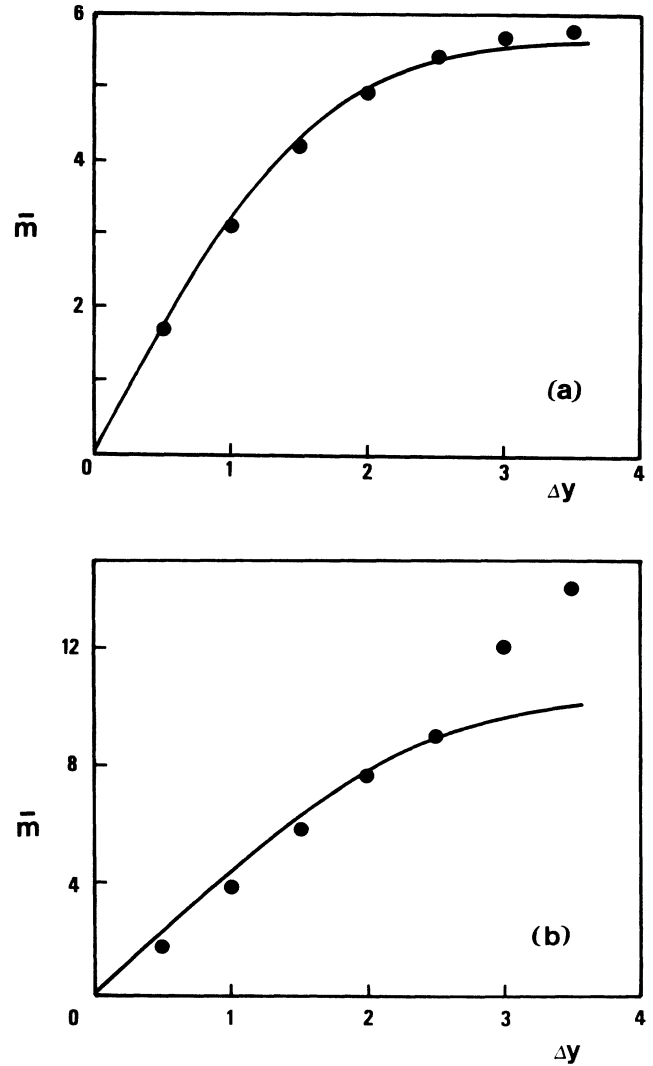


FIG. 2. Average charged multiplicity \bar{m} as a function of rapidity intervals Δy for $p + \text{Xe}$ collision at 200 GeV: (a) for the forward hemisphere, and (b) for the backward hemisphere. The experimental data are taken from Ref. 10 and the solid line is the result of our model.

the interval between y_c and $y_c \pm \Delta y$. However, since the effective target is certainly *not* a single nucleon, it is somewhat misleading to think of y_c as any "center of mass"; instead, one should simply think of y as rapidities in the laboratory frame, arbitrarily shifted by 3.0 units. We see that the agreement in $\bar{m}(\Delta y)$ is good except for large rapidities in the backward hemisphere, corresponding to $y \sim 0$ in the laboratory. The reason for the discrepancy lies not so much in the theoretical model as in a different convention between the two reported measurements. The data in Fig. 1 correspond to the "produced" particles in Ref. 8, which exclude slow protons "evaporated" from the nucleus, while the data in Fig. 2

have not been subjected to a similar cut. The contamination by the "evaporated" protons is responsible for the extra particles detected near $y \sim 0$ in the laboratory frame.

Figure 3 shows the distribution $P(m, \Delta y)$ for the number of charged particles in different rapidity windows; again, except for the largest windows in the backward hemisphere, the agreement is excellent. Some fits enjoy a comparable degree of success for these distributions employ one or more parameters (e.g., the two parameters of the negative-binomial distribution) for *each* of these curves,^{10,11} which would be not nearly as stringent a test as the model here, which employs only three marginally adjustable parameters to describe *all* of Figs. 1-3.

The attribution of the discrepancy to "evaporated" protons can be tested by considering the negative charges, which are free from such contamination. Figure

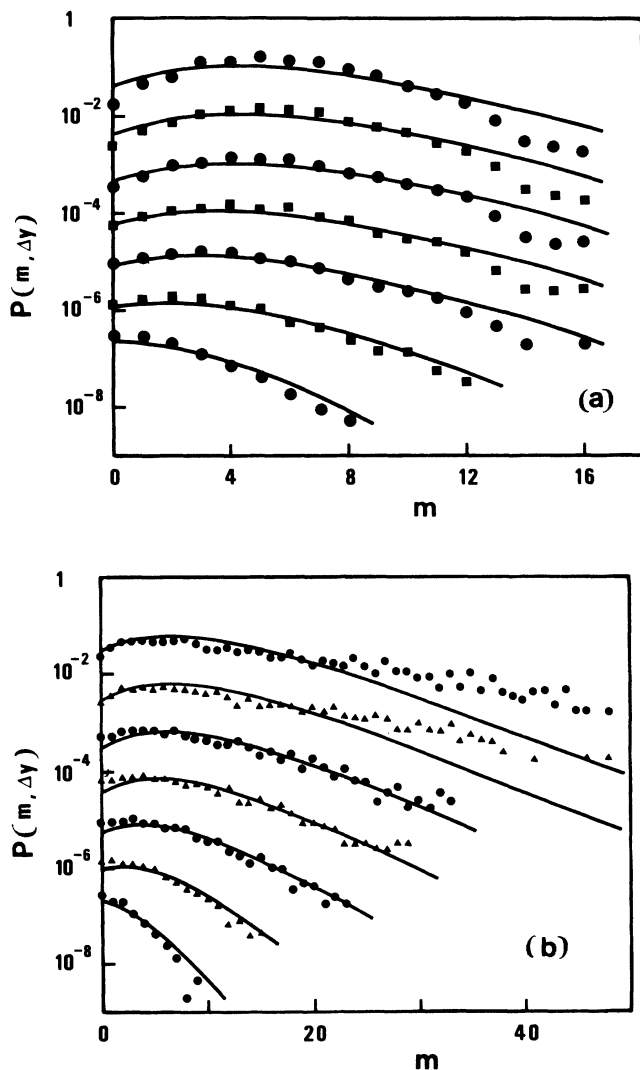


FIG. 3. The multiplicity distribution $P(m, \Delta y)$ for all charged particles in various rapidity intervals Δy for $p + \text{Xe}$ collision at 200 GeV. The data (Ref. 10) for the largest rapidity interval are referred to the vertical scale shown, and each consecutive one is scaled down by an additional factor of 10: (a) for the forward hemisphere and (b) for the backward hemisphere. The intervals from the top to bottom are $\Delta y = 3.5, 3.0, 2.5, 2.0, 1.5, 1.0, 0.5$. Our results are shown by the solid lines.

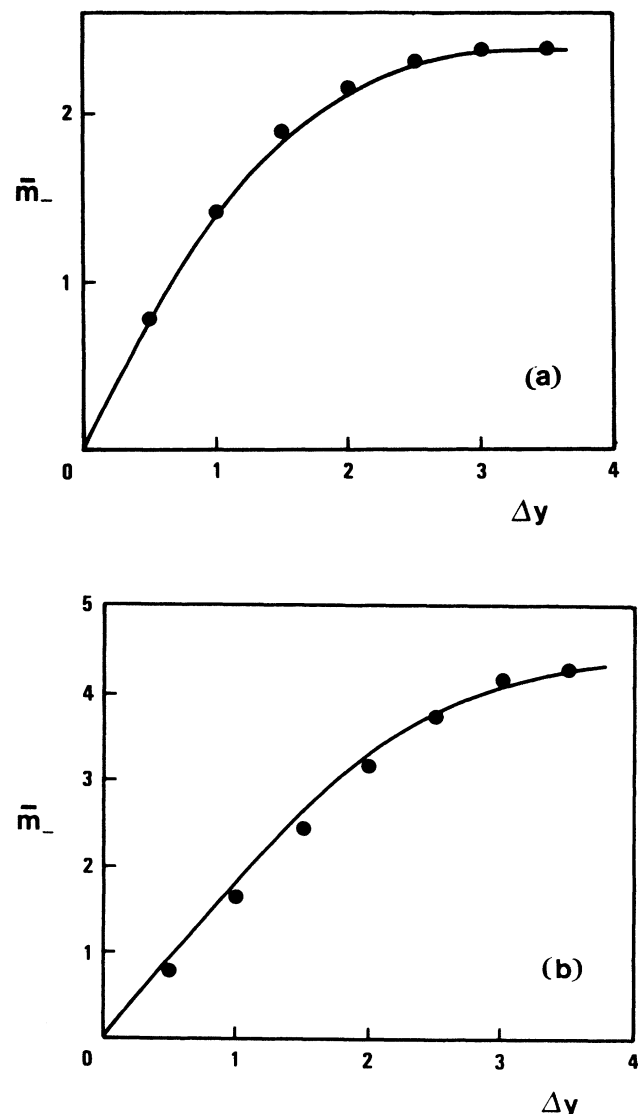


FIG. 4. Same as Fig. 2, but for negative multiplicity \bar{m}_- in $p + \text{Xe}$ collision.

4 shows $\bar{m}_-(\Delta y)$, while Fig. 5 shows the distribution $P_-(m_-, \Delta y)$, both calculated without any further adjustable parameters. The fit is excellent.

Next consider the reaction $p + \text{Au}$ at 360 GeV;¹¹ the analogous results for $p + \text{Al}$ will not be shown. Unfortunately in this case there are no data with a cut on “evaporated” protons, and we are forced to apply our model to all the charged particle, “produced” and “evaporated.” Since the latter are not expected to have thermalized (which may be taken as the definition of “evaporated”), we expect the simple-minded thermodynamic model to be somewhat less accurate.

The parameters chosen are $f = 2.0$, $h = 0.65$, $k = 0.69$, and the fit to $\bar{m}(\Delta y)$ is shown in Fig. 6, with reasonable agreement. The agreement for $P(m, \Delta y)$, is also good, as seen from Fig. 7.

The minor differences in the fitted values of h and k from the previous example are probably not significant, but the considerably larger value of f (2.0 vs 1.3) is expected, because the two sets of data have different cuts.

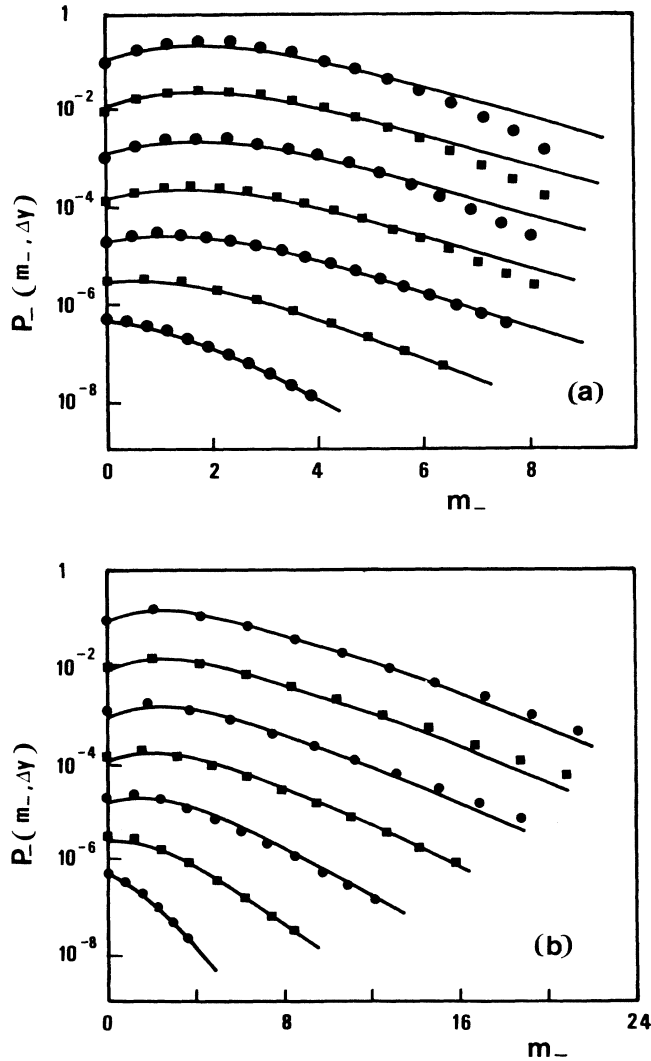


FIG. 5. Same as Fig. 3, but for negative-multiplicity distribution $P_-(m_-, \Delta y)$.

The beam particle (and its fragments) interact strongly with a relatively narrow tube (area = $f_1\sigma$, $f_1 \sim 1.3$), but also deliver a small amount of energy to the surrounding “spectator” nucleons, causing the latter to “evaporate.” Thus if there is no cut on the “evaporated” protons, the weaker interaction with the surrounding nucleons would be included, and the effective target would be a broader tube (area = $f_2\sigma$, $f_2 \sim 2.0$).

IV. CONCLUSION

We have obtained good fits to the data by using very simple ideas and only three parameters, none of which can be significantly adjusted. The ideas are consistent with those used in hh scattering. Of course, the fit can be further improved by making the model more sophisticated, e.g., allowing h to vary with impact parameter, but

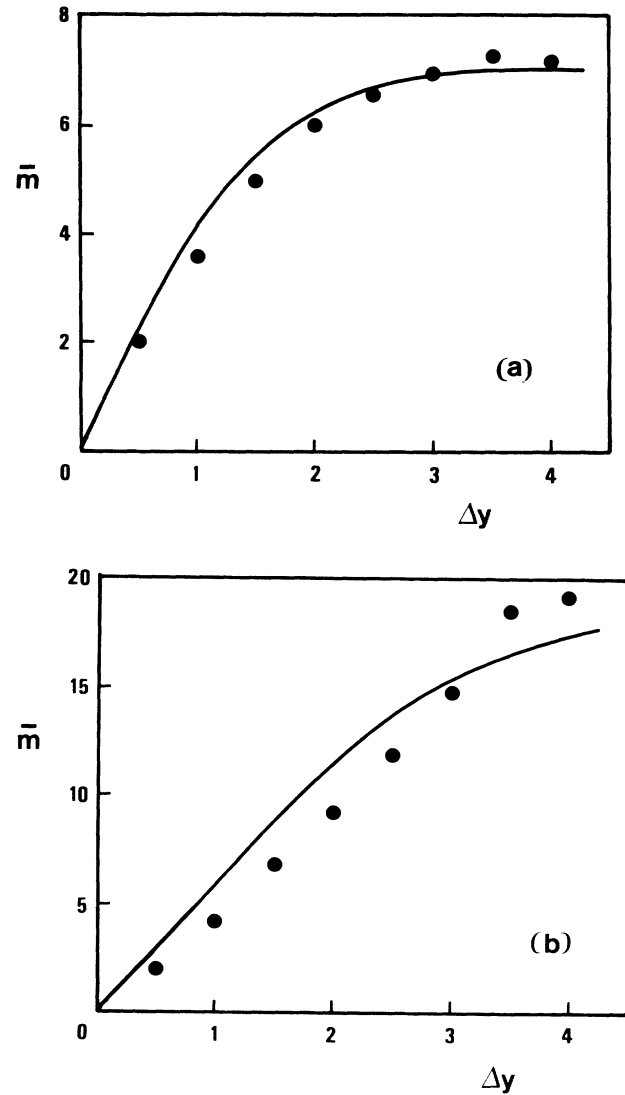


FIG. 6. Average charged multiplicity \bar{m} as a function of rapidity intervals Δy for $p + \text{Au}$ collision at 360 GeV: (a) for the forward hemisphere, and (b) for the backward hemisphere. The solid line is our fitted result with $f = 2.0$, $h = 0.65$, and $k = 0.69$, compared with the experimental data (Ref. 11).

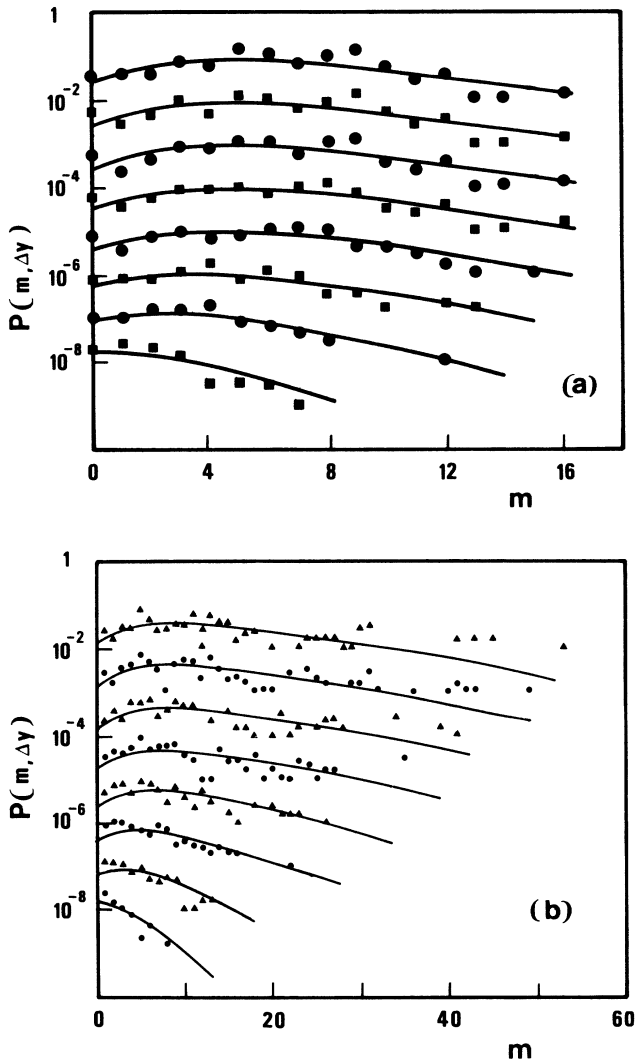


FIG. 7. Same as Fig. 3, but for $p + Au$ collision at 360 GeV, data from Ref. 11. The intervals from the top to bottom are $\Delta y = 4.0, 3.5, 3.0, 2.5, 2.0, 1.5, 1.0, 0.5$.

that is not the point of the present investigation. The lesson to be drawn is that the main features of the data are determined by very general considerations, essentially of a kinematic nature. In particular, the conservation of momentum is important in controlling the asymmetry between forward and backward hemispheres (a feature absent from hh scattering with colliding beams), and the different dynamical models which have been successful all share the properties that (a) there are $\sim \nu$ collisions and (b) the collisions conserve momentum. We argue that it is these particular properties, rather than the dynamical framework, which have been confirmed by the data. In saying so, we do not imply that any of these dynamical models is ruled out.

However, the success of thermodynamic ideas would tend to cast doubt on one class of models, namely, those in which the final state “remembers” some vestige of the initial colliding system (apart from the leading particles, on the one hand, and the spectator nucleons, on the other), such as certain versions of the two-fireball models.³⁵ The very essence of thermodynamics is that the system, through strong interactions, “forgets” everything about the initial state apart from conserved quantities, in this case net charge, total energy and total momentum. This concept is already implicit in early parton ideas,³⁶ in which the central region in the one-particle inclusive distribution is regarded as neutral and independent of the nature of the beam and target particles.

In short, we claim that the main features of the data can be understood without specifying the detailed dynamics, while, on the other hand, to discriminate between different dynamical models would require examination of the finer aspects of the data, such as correlations.

ACKNOWLEDGMENTS

We thank C. S. Lam, W. Chen, and E. Yen for several discussions. This work was partially supported by an operating grant from the Natural Sciences and Engineering Council of Canada. T.O. thanks the Killam Trustees for financial support.

- ¹E. L. Feinberg, Zh. Eksp. Teor. Fiz. **50**, 202 (1966) [Sov. Phys. JETP **23**, 132 (1966)]; K. Gottfried, Phys. Rev. Lett. **32**, 957 (1974).
- ²K. S. Kolbig and B. Margolis, Nucl. Phys. **B6**, 85 (1968); C. Bemporad *et al.*, *ibid.* **B33**, 397 (1971); A. S. Goldhaber, Phys. Rev. D **7**, 765 (1973).
- ³H. I. Miettinen and J. Pumplin, Phys. Rev. Lett. **42**, 204 (1979); K. Young, Phys. Rev. D **22**, 2275 (1980); **25**, 761 (1982).
- ⁴L. Van Hove, Phys. Lett. **118B**, 138 (1982); *Quark Matter '86*, proceedings of the Fifth International Conference on Ultrarelativistic Nucleus-Nucleus Collisions, Asilomar, California, 1986, edited by L. Schroeder and M. Gyulassy [Nucl. Phys. **A461**, Nos. 1 and 2 (1987)]; *Quark Matter '87*, proceedings of the Sixth International Conference on Ultrarelativistic Nucleus-Nucleus Collisions, Munster, West Germany, 1987, edited by H. Satz, H. J. Specht, and R. Stock [Z. Phys. C **38** (1988)].
- ⁵NA35 Collaboration, J. Bartke, in *Proceedings of the XXIV International Conference on High Energy Physics*, Munich, West

- Germany, 1988, edited by R. Kotthaus and J. Kuhn (Springer, Berlin, 1988); NA35 Collaboration, A. Bamberger *et al.*, Phys. Lett. B **205**, 583 (1988); WA80 Collaboration, I. Lund *et al.*, Z. Phys. C **38**, 51 (1988); E802 Collaboration, L. P. Remsberg and M. J. Tannenbaum *et al.*, *ibid.* **38**, 35 (1988); NA35 Collaboration, A. Bamberger *et al.*, Phys. Lett. B **184**, 271 (1987); NA35 Collaboration, T. H. Humanic, in *Proceedings of the International Europhysics Conference on High-Energy Physics*, Uppsala, Sweden, 1987, edited by O. Botner (Uppsala University, Uppsala, Sweden), p. 137.
- ⁶J. Babecki and G. Novak, Acta Phys. Pol. **B9**, 401 (1978); E. Stenlund and I. Otterlund, Nucl. Phys. **B198**, 407 (1982); M. K. Hegab and J. Hüfner, Phys. Lett. **105B**, 103 (1981); N. Suzuki, Nucl. Phys. **A403**, 553 (1983).
- ⁷N. N. Biswas *et al.*, Phys. Rev. D **33**, 3167 (1986).
- ⁸C. De Marzo *et al.*, Phys. Rev. D **26**, 1019 (1982).
- ⁹J. L. Bailly *et al.*, Z. Phys. C **35**, 301 (1987).
- ¹⁰F. Dengler *et al.*, Z. Phys. C **33**, 187 (1986).
- ¹¹J. L. Bailly *et al.*, Z. Phys. C **40**, 215 (1988).

- ¹²X. Cai, W. Q. Chao, and T. C. Meng, *Phys. Rev. D* **36**, 2009 (1987).
- ¹³K. Werner, *Phys. Rev. D* **39**, 780 (1989).
- ¹⁴C. S. Lam, D. Kiang, and T. Ochiai, *Int. J. Mod. Phys. A* **5**, 2411 (1990).
- ¹⁵R. C. Hwa and X. N. Wang, *Phys. Rev. D* **39**, 2561 (1989); X. N. Wang and R. C. Hwa, *ibid.* **39**, 2573 (1989).
- ¹⁶D. Kiang, S. H. Ling, K. Young, and C. S. Lam, *Phys. Rev. D* **31**, 31 (1985).
- ¹⁷R. J. Glauber, in *Lectures in Theoretical Physics*, edited by W. E. Brittin and L. G. Dunham (Interscience, New York, 1959).
- ¹⁸U. Amaldi, in *High Energy Collisions—1973 (Stony Brook)*, proceedings of the Fifth International Conference, Stony Brook, New York, edited by C. Quigg (AIP Conf. Proc. No. 15) (AIP, New York, 1973), p. 47.
- ¹⁹W. Q. Chao, M. K. Hegab, and J. Hufner, *Nucl. Phys.* **A395**, 482 (1983).
- ²⁰W. Thomé *et al.*, *Nucl. Phys.* **B129**, 365 (1977).
- ²¹A. Bialas, M. Bleszyński, and W. Czyz, *Nucl. Phys.* **B111**, 461 (1976); I. Otterlund and E. Stenlund, *Phys. Scr.* **22**, 15 (1980).
- ²²Z. Koba, H. B. Nielsen, and P. Olesen, *Nucl. Phys.* **B40**, 317 (1972).
- ²³M. Le Bellae, J. L. Meunier, and G. Plant, *Nucl. Phys.* **B62**, 350 (1973); T. T. Chou and C. N. Yang, *Phys. Lett.* **116B**, 301 (1982); C. S. Lam and P. S. Yeung, *ibid.* **119B**, 445 (1982).
- ²⁴S. H. Ling and K. Young, *Can. J. Phys.* **63**, 954 (1985).
- ²⁵D. Kiang, T. Ochiai, Y. P. Chan, and K. Young, *Can. J. Phys.* **68**, 145 (1990).
- ²⁶P. Slattery, *Phys. Rev. Lett.* **29**, 1624 (1972).
- ²⁷M. M. Aggarwal *et al.*, *Phys. Rev. D* **29**, 150 (1984).
- ²⁸In practice, measured only against rapidity or pseudorapidity.
- ²⁹E. Fermi, *Prog. Theor. Phys.* **5**, 570 (1950); L. D. Landau, *Izv. Akad. Nauk. SSSR, Ser. Fiz.* **17**, 51 (1953).
- ³⁰T. T. Chou, C. N. Yang, and E. Yen, *Phys. Rev. Lett.* **54**, 510 (1985); T. T. Chou and C. N. Yang, *Phys. Rev. D* **32**, 1692 (1985).
- ³¹T. S. Li and K. Young, *Phys. Rev. D* **34**, 142 (1986).
- ³²A. Capella and A. Krzywicki, *Phys. Rev. D* **18**, 3357 (1978); A. Capella and J. Tran Thanh Van, *Phys. Lett.* **93B**, 146 (1980).
- ³³N. N. Nikolaev and A. Ya Ostapchuck, *Lett. Nuovo Cimento* **23**, 273 (1978); a simple statement of this model is provided in Ref. 19.
- ³⁴T. S. Li and K. Young, *Mod. Phys. Lett. A* **2**, 41 (1987).
- ³⁵See, e.g., R. K. Adair, *Phys. Rev. D* **5**, 1105 (1972).
- ³⁶See, e.g., R. P. Feynman, *Photon-Hadron Interaction* (Benjamin, New York, 1972).